



Article

Use of AMT Transformers and Distributed Storage Systems to Enhance Electrical Feeding Systems for Tramways

Romano Giglioli, Giovanni Lutzemberger *  and Luca Sani 

Department of Energy, Systems, Territory and Constructions, University of Pisa, 56122 Pisa, Italy; romano.giglioli@unipi.it (R.G.); luca.sani@unipi.it (L.S.)

* Correspondence: giovanni.lutzemberger@unipi.it; Tel.: +39-050-221-7311

Received: 18 August 2020; Accepted: 8 September 2020; Published: 10 September 2020



Abstract: Tramway systems are more and more diffused today, to reduce pollution and greenhouse emissions. However, their electrical feeding substations can have significant margin for improvement. Therefore, it is questionable which kind of changes can be introduced, by changing their main features. First of all, transformer technology can be enhanced, by moving from the standard transformer to the amorphous metal one; thus, guaranteeing a significant reduction in losses. Then, by installing one dedicated storage systems for each substation. This solution can help to increase the energy efficiency; thus, recovering the tram braking energy and reducing the delivered energy from the grid, and also the reliability of the system; thus, guarantee different levels of services, in the case of failure of a feeding substation. This paper investigates in a systematic approach the two proposed solutions. In particular an amorphous metal transformer has been properly designed, and performance compared to the standard one. Then, evaluation of distributed storage installation was performed, and the aspects of reliability for these systems evaluated. Results have shown the general feasibility of the proposed solutions, showing a significant energy saving with respect to the conventional ones.

Keywords: amorphous transformer; energy storage; failure; feeding substation; tramway

1. Introduction

Tramway systems are more and more diffused today, in order to limit environmental impact from transportation field. However, their electrical feeding substations show significant margin for improvements by introduction of new features, to improve their technical characteristics.

Firstly, feeding system solutions typically do not allow the reversibility of power fluxes from electrical feeding substations (ESSs). Therefore, the braking energy can be recovered only by other trains running, when available to do that (e.g., during acceleration or constant speed phases). As deeply investigated in [1–4], if some storage capability is used, the amount of the energy to recover can be significantly enhanced.

Another option typically considered in the literature is the use of bidirectional feeding substations without any storage capability, as described in [5]. However, we must consider that in this case the amount of the recoverable energy is slightly reduced, since losses increase due to the high distances to be covered. Additionally, the absence of storage capability does not help in improving the system reliability, and the overall cost of the system is very high due to its complexity.

If non-reversible feeding substations equipped with storage are considered, the authors already did the calculation of the energy saving derived from introduction of some stationary storage systems on an existing tramway, through a simulation tool specifically developed in Modelica language, which include the electrical network, the vehicles, and the driver [6]. This tool has been validated

through the experimental measurements collected from an existing tramway and outputs crosschecked also with results given by different tools, in different case studies [7]. Once developed and properly set, the tool has allowed to demonstrate, from the evaluation of the annual demand of electricity from electrical feeding substations (ESSs), the cost-effectiveness due the introduction of a limited number of storage systems, allowing a payback time shorter with respect to the useful plant life [8,9]. However, it can be of interest to analyze if the number of installed storages can further increase with respect to what already studied, up to the installation of one storage for each electrical feeding substation (ESS), in order to increase the system reliability and to guarantee adequate levels of redundancy in the case of failure of one or more electrical feeding substations (ESSs). Additionally, when they are installed on each substation, they can also reduce the size of the transformers, since they are able to sustain peaks of power requested by the different trains on track. These aspects will be widely analyzed in this paper.

Additionally, the extensive campaign of measurements also has shown the high amount of losses caused by the transformers linked to the MV network. Starting from this, a deep analysis about component technologies inside each electrical feeding substation (ESS) was carried out. In particular, utilization of the amorphous core transformer (AMT) was considered, by designing a customized version for the considered application, in order to improve efficiency and thus verifying how much losses can be reduced.

This paper therefore shows how to systematically improve the electrical feeding substations (ESSs) from the point of view of the electrical energy utilization, moving from the improvement of the transformer technology and of the solutions regarding stationary storage systems, within a cost-effectiveness perspective.

2. Technology Improvements

2.1. Transformer

In a standard electrical feeding substation (ESS), a three-phase distribution transformer with two LV windings, star, and delta, and a MV delta winding, is typically used. It is manufactured so there is no phase displacement between the MV secondary winding and the LV delta winding and hence the star LV secondary winding leads the MV winding by 30° . Each LV winding is then connected to a converter's bridge [10].

This transformer typology, as all electrical machines, has losses in the windings (in losses), due to the current circulation, and in the iron (no-load losses) due to magnetic hysteresis and eddy currents. Although the latter are a small fraction, their contribution in energy is not negligible compared to load losses because the transformer is always connected to the network and then subjected to the grid voltage almost constant over time: thus their no load losses remain unchanged. Except for densely populated urban centers, the average power delivered by a MV/LV transformer, during a week, is less than 40% of the nominal power. This value is reduced to 10% at night. A cabin transformer generally is oversized to compensate for, in the future, any increase of the output power, taking into account that the average useful life exceeds thirty years. Load losses, by following the same trend, are therefore always lower than the nominal one. All this explains the interest in industry and regulations, regarding the realization of machines with lower iron losses. In the joint overlap regions, the losses increase around 50% due to interlaminar flux and deviation of flux from rolling direction.

In the case of converter transformer, under normal operating conditions, the current in the windings has a stepped waveform. For a 12-pulse operating condition, the converters create harmonic of order $12k \pm 1$, where k is integer, at the HV side. The presence of harmonics is one of the most severe aspect of the converter transformer. Harmonics increase eddy losses in the windings and stray losses in structural elements of the converter transformer. In addition, due the asymmetries in valve firing angles in the converter, the currents in the transformer windings have a DC component. In order to minimize excessive losses and noise, an accurate design of the magnetic circuit is needed.

Transformers distribution (with the high voltage (HV) less than 24 kV and oil cooling) are classified according to IEC 50464-1 based on the rated power and divided into subclasses according to the value of no-load losses (five classes from A_0 to E_0) and load losses (four classes from A_k to D_k). The state of the art is represented by machines in class $C_k A_0$.

Regulation 548/2014 of the European directive in 2009 defined the minimum efficiency requirements and deadlines for new distribution transformers placed on the European market: class $A_k A_0$ from July 2021 [11]. Currently in Europe, the power transformers core is made with regular grain-oriented (RGO) silicon steel. This technology is sufficiently mature so that the achievement of greater efficiency classes may be obtained only by decreasing the current density in the coils and the magnetic induction in the cores, increasing the volume of the transformer. Furthermore, the production process has a low degree of automation. Considering this background, the request for high efficiency transformers could increase significantly in the future; therefore, the excellent market perspective for these machines is evident.

A really interesting solution is the amorphous metal transformer (AMT). It was introduced in the US market (in the mid-1980s), and in Southeast Asia (Japan and China) during the last decade. The amorphous metal is a metallic alloy of iron, boron, and silicon (Fe-B-Si) made by solidifying alloy melts at rates rapid enough to prevent the metal crystallization [12,13]. Such rapid solidification leaves a vitrified solid with a random (amorphous) atomic structure. The high heat extraction rates constrain the solid in the form of a thin ribbon, about 25 μm thick. Due to the presence of boron, amorphous metal has a reduced saturation induction than RGO steel. As result, amorphous core transformers often have a larger core cross-sectional area, resulting in larger coils and transformer footprint. The most significant characteristic of an amorphous metal in a transformer is that it yields a much lower core loss than even the best grades of RGO steel, by up to 70% [14].

Since the amorphous ribbon does not have a mechanical stiffness, the transformer core no longer has the function of holding up the coils. As a result, the structural design of this machine is significantly different compared to a transformer with RGO silicon steels, as shown in Figure 1a.

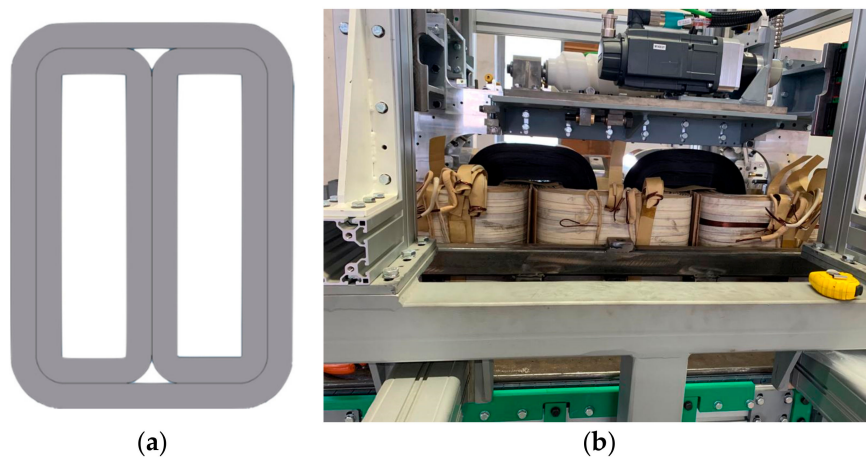


Figure 1. Three-legged transformer core made by amorphous alloy (a); transformer continuous core [15] during the automated manufacturing process (b).

Due to their significant different mechanical properties, another transformer manufacturing technique is also needed. Since the material is thin, the application of amorphous metal is restricted to wound transformer cores. Until now, the solution has been a wound core with distributed gaps: the ends of each ribbon are lapped with each other. The flux concentrations in the neighborhood of the joint gaps cause additional iron losses.

By exploiting the mechanical characteristics (flexibility) of ribbon [15] proposes an innovative assembly process for wound ferromagnetic core in which the joint gaps are eliminated, as in Figure 1b. All this, in addition to further improvement of the efficiency, will ensure a high standard product.

The technological innovation consists in being able to wind up a ribbon of magnetic material directly into the preformed coils. In particular the originality consists in providing a removable automated system, constituted by a series of rolls, on which the thin sheet of amorphous material is wound (with a thin layer of thermosetting resin deposit), mounted on a motorized guide with an optimized shape. The shape is a closed loop (rectangular with rounded corners or elliptical) formed around the coils.

The production process is completely different from the one currently used for the production of core laminations, and the solution developed will allow to introduce a high degree of automation, so that the productivity of its plants can be significantly increased.

Typically, an AMT is always more expensive than a silicon steel unit but can be more economical in many power systems. To specify cost-effective transformer performance, utility engineers commonly use a “loss-evaluation” method. This approach considers transformer loading patterns, energy costs, inflation, interest rates, and other economic factors to calculate the net present value of a watt of electric power. The combination of the initial cost of the transformer with its cost of operation, is summarized by the total owning cost (TOC) [16]:

$$TOC = B_P + (A \cdot C_L) + (B \cdot L_L) \quad (1)$$

where B_P is the bid price, A is the core loss factor, C_L are the core losses (e.g., losses occurring in the magnetic core, due to alternating magnetization), B is the Load Loss Factor, and L_L are the load losses (e.g., losses when load currents flow). In the case of energy costs sufficiently high, AMTs make economic as well as environmental sense.

2.2. Storage System

As said, a train can send its braking energy on the catenary, only in the vicinity of other trains running, available to adsorb that energy. Therefore, when a stationary storage system is introduced, energy recovery is enhanced. In this way, also when no other trains are present, the storage system can adsorb the energy from the trains engaged in braking, and delivering it at a different time, in the presence of enough load. A detailed description of the problem, together with evaluation of the energy saving from electrical feeding substations, is widely described in [6,8,9]. The storage is normally not directly linked to the grid, but it is interfaced through the use of a DC/DC converter, having different functionalities: first of all, it is possible to control the energy flows; thus, preserving the storage system by the delivery or adsorption of high current peaks. Then, SOC drift can be avoided; therefore, maintaining the battery at an intermediate SOC value; thus, avoiding progressive charging or discharging, leaving it able to recover or deliver energy. Finally, to guarantee flexibility in the storage sizing, having the battery voltage not dependent from the operating pantograph voltage.

At least in theory, each electrical feeding substation (ESS) can be equipped with its dedicated storage or, to reduce costs, just a few storage systems can be installed, in correspondence to one or a few more substations. Certainly, when the number of storage systems equals the number of the feeding substations (ESSs), it is possible to reduce the sizing of the transformer, e.g., up to half of the original power, since the extra-power needed can be delivered by the storage systems.

This aspect, also by guaranteeing a reduction of the transformer TOC, as general rule, can therefore compensate, or at least cancel, the extra-costs needed for the storage systems. Additionally, extra-services can also be provided, by guaranteeing the train are at least able to reach the nearest train stop, in the case of failures of one or more ESSs. In this way, system reliability is enhanced, and adequate levels of redundancy are given.

Another aspect of interest is given by the technology used for the application. In fact, many lithium-based technologies are today available. One of the most common, based on utilization of lithium-iron-phosphate (LFP) cells [17], considered also in [8,9], which are typically considered in energy-oriented applications, and characterized by very low costs. In the last years, other technologies have been more and more considered, much more oriented in delivering or adsorbing high powers for short time durations. In particular lithium-titanate (LTO) cells [18] are specifically power-oriented, and therefore aligned to the application requirements, in which high current peaks have to be adsorbed during the regenerative braking of the trains. In fact, according to authors experience and manufacturer indications [18], they are able to sustain high charging or discharging current peaks, in the order of ten times their nominal capacity, for several tens of thousands of cycles; thus, showing also a significant life resistance to number of cycles.

3. The System Under Study

3.1. Architecture

The system under analysis is in Bergamo (Italy). The pattern has a full length of 12 km, and it is characterized by 10 feeding electrical substations (ESSs), whose positions are in Figure 2.

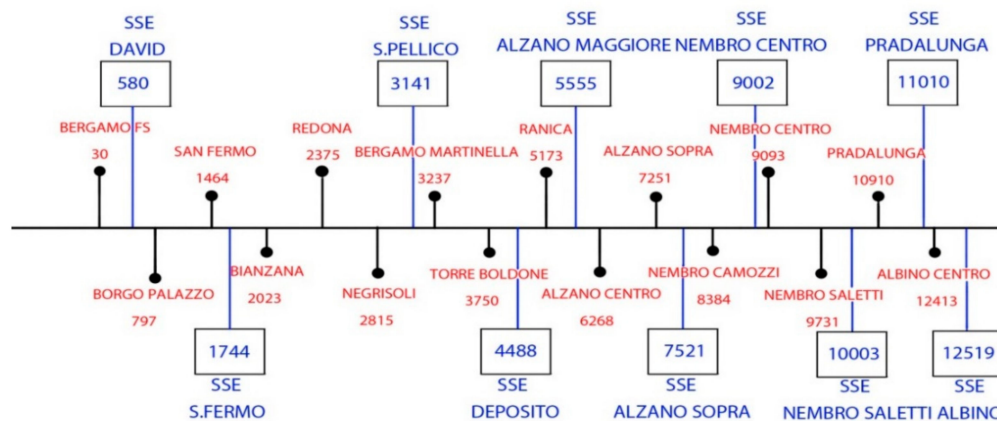


Figure 2. Position of the electrical feeding substations (ESSs) in blue and stops in red along the path (distances from the terminal are indicated in meters).

The main technical data of this system are in the next Table 1.

Table 1. Main features of the system.

Tram	
Empty Mass (t)	41.9
Load mass (t)	17.4
Max power (kW)	628
Max tractive force (kN)	72.1
Max speed (km/h)	70
Electrical Feeding Substations	
Medium voltage (kV)	15
Output No load DC voltage (V)	798
Max power (MW)	2.0

The feeding supply system is schematically represented in the next Figure 3. How visible, each ESS has a MV/LV transformer (TR1) with its converter, in order to feed energy needed for propulsion. Then, a second transformer (TR2) feeds the LV auxiliary loads, e.g., visual and acoustic signals of each ESS and of the nearest train stop. As always depicted in Figure 3, energy meters were installed in each ESS

to measure energy flows, and also additional data logger were introduced, to measure instantaneous DC voltage and current. Measurement devices are also indicated in Figure 3.

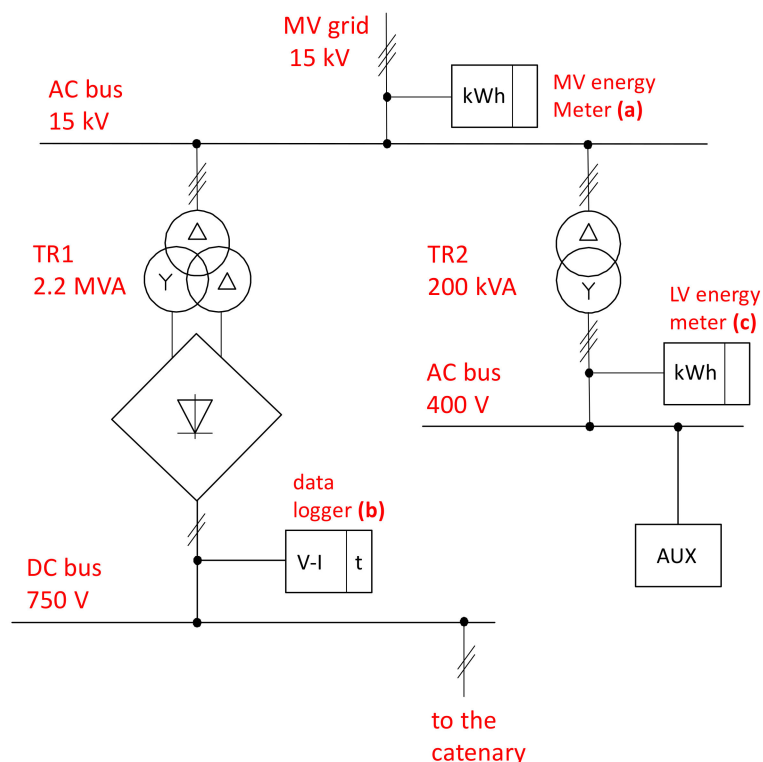


Figure 3. Scheme of ESS, including measurement system.

The main characteristics of the transformer TR1 are in the next Table 2.

Table 2. Main parameters of the standard transformer (TR1).

Rated Power	2.2 MVA
Voltage (primary/secondary)	15/04 kV
Number of primary windings	1 (Delta)
Number of secondary windings	2 (Star-Delta)
Vector group	Dy11d0
Medium	Dry
Iron core Layout	Three limbs
Iron core Material	Cold-rolled grain-oriented steel (CRGO)
Winding material	Copper
Maximum load losses P_k	17.5 kW
Maximum no-load losses P_0	4.5 kW
Efficiency at full load	0.990

3.2. Energy Flows

Campaign of measurements accurately described in [8] allows to evaluate how energy fluxes are divided between losses of the devices in each ESS, energy demands of the trains, e.g., the energy needed for traction and for on-board auxiliary loads, and the energy required by LV auxiliary loads. Moreover, these measurements have been performed considering the real number of trains in operation, variable depending on the considered day. In this way, school working days, having some hours

per day characterized by ten trains in operation, no-school working days, in which five trains are in operation, and finally holidays, having just three trains on track. Additionally, also effects of the season were considered, e.g., having different contributions from heating or air conditioning systems. Results for a mid-season no-school working day, in the case of three ESSs, are in the next Table 3. Energy losses are in the range 20–24%. Further details are in [8,9].

Table 3. Daily energy flows for three ESSs.

ESSs	Daily Energy MV (kWh)	Aux Energy LV (%) ¹	ESS Losses (%) ¹	Traction Energy (%) ¹
San Fermo	1231	16.3	18.4	65.3
Alzano	882	22.3	22.4	55.3
Albino	1167	10.8	18.5	70.7

¹ Related to the corresponding daily MV energy.

As further step, yearly consumptions have been measured, and shown in the next Table 4. The full energy consumption from MV is shared between energy demand for traction, losses and LV auxiliary loads.

Table 4. Annual energy demand.

Energy from ESSs (MWh/y)	
Total MV Energy (a)	4100
Traction (b)	2756
LV Aux Energy (c)	738
Losses	606

How visible, annual energy losses from the transformer and its dedicated converter are about 15% of the total MV energy demand. It is therefore needed an accurate in-depth analysis of the standard transformer losses, thus evaluating the benefits given by utilization of the amorphous core transformer technology (AMT).

4. The Amorphous Metal Transformer (AMT)

4.1. Design of the Transformer

In order to improve the system reliability, the transformer TR1 can be replaced by two identical transformers having half power (i.e., 1100 kVA), in parallel connection. The main aim of the activity was therefore the design of a 1100 kVA AMT transformer, having one primary and two secondary windings.

First of all, starting from the architecture depicted in Figure 1a, it has been made the analytical winding size, then moving to the CAD modelling and finally the FEM analysis. Main parameters of the 1100 kVA rectifier transformer with amorphous alloy core have been finally summarized in the next Table 5. The design is compliance with EN-60146–1-3. The rated voltage and currents in primary and secondary windings of the transformer are 15 kV/0.4 kV and 42 A/538 A, respectively.

The operating flux density in the transformer core is fixed around 1.6 T to mitigate the effects of harmonics and dc component of the winding current. Due to the shape of the amorphous alloy strip, the cross section of the core is generally made rectangular, and the winding is also made rectangular. Delta and star LV windings are insulated from one another. MV windings are wrapped between the LV windings. Usually, LV windings are foil wound and MV may be windings disc wound. Both are made by aluminum.

As remarked, the detailed 3D FEM analysis has been carried out in order to validate the design of the transformer by using Simcenter Magnet software [19].

Table 5. Main parameters of 1100 kVA amorphous core transformer (AMT) transformer.

Rated Power	1.1 MVA
Voltage (primary/secondary)	15/04 kV
Number of primary windings	1 (Delta)
Number of secondary windings	2 (Star–Delta)
Vector group	Dy11d0
Medium	Dry
Iron core Layout	Three limbs
Iron core Material	Amorphous Metglass 2600
Weight	2200 kg
W × H × D	1100 mm × 1500 mm × 284 mm
Winding material	Aluminum
Core mass	980 kg
Magnetic flux density	1.4 T
V _{cc} %	3.5 %
Maximum load losses P _k	6.0 kW
Maximum no-load losses P ₀	0.6 kW
Efficiency at full load	0.9924

4.2. Application to the Tramway System

After designing the AMT transformer, it is important to evaluate which help this latter can guarantee on the full amount of energy consumption evaluation, as in the previous Table 4. Tables 2 and 5 show that both load and no-load losses are reduced. In detail, load losses are decreased from 17.5 kW to 12 kW in the case of two AMT transformers connected in parallel, while a significant reduction concerns the no-load losses, moving from 4.5 kW to 1.2 kW. Although these values are negligible with respect to the load losses amount, we must consider that they occur on the full number of hours per day, while load losses are present only in the average period of use. This is because, it is therefore needed to calculate through a weighted average the effects of the contributions of losses. In particular, we can consider what is currently shown in Equation (2).

$$L_{tot} = n_t \cdot n_d \cdot (t_{CL} \cdot C_L + t_{LL} \cdot L_L) \quad (2)$$

where L_{tot} is the full amount of losses per year given by utilization of standard transformers, n_t is the number of the transformers, n_d is the operative number of days per year, C_L are the core power losses calculated for the time duration t_{CL} , i.e., equal to 24 h/day, L_L are the full load losses, calculated for the average time duration t_{LL} . Moving from the previous experimental evaluation of losses, for which 606 MWh/y were measured (see Table 4), and by using data of standard transformers, i.e., having C_L and L_L respectively equal to 4.5 kW and 17 kW, it was then possible to obtain the average time duration t_{LL} by utilization of Equation (2). It was finally considered 10 installed transformers, and 8760 operative hours per year. In particular, we obtained:

$$t_{LL} = \frac{L_{tot}}{n_t \cdot n_d \cdot L_L} - \frac{t_{CL} \cdot C_L}{L_L} = 3.4 \text{ h/day} \quad (3)$$

Moving from this, relation Equation (2) was newly adopted, by changing C_L and L_L to the values of the AMT transformers, e.g., 1.2 kW and 12 kW, respectively (see Table 4), and by taking unmodified the previously time durations. With the new sizing for the transformer, and by taking unmodified the

architecture of Figure 3, losses changes from 606 MWh/y to 254 MWh/y; thus, having a 58% reduction. Therefore, by taking the same requests for traction (e.g., 2756 MWh/y) and auxiliary loads (738 MWh/y), the total MV energy request is reduced to 3748 MWh/y.

In conclusion, the total MV energy shows an 8% reduction, and losses are about 7% of the total MV energy demand. The amount of losses are therefore considerably reduced compared to before. This is visible also from Equation (1). In fact, TOC reduction is about 20% than for the standard transformer.

It is finally questionable if also the TR2 transformer, aimed to feed auxiliary loads, could be replaced with the introduction of a second AMT transformer. However, its reduced power (i.e., 200 kVA with respect to 2.2 MVA) would make a negligible reduction in the LV aux energy spent, if an equivalent improvement of efficiency as for the TR1 would be considered, in the order of a few MW per year.

5. Storage System Integration

5.1. Storage System Sizing

The architecture of each ESS, when equipped with some storage capability, in the next Figure 4, while the final sizing of the considered stationary storage system is instead shown in Table 6. The first rows show the two different lithium-based technologies which have been considered. The first one is based on LFP cells [17], while the second one is based on LTO cells [18].

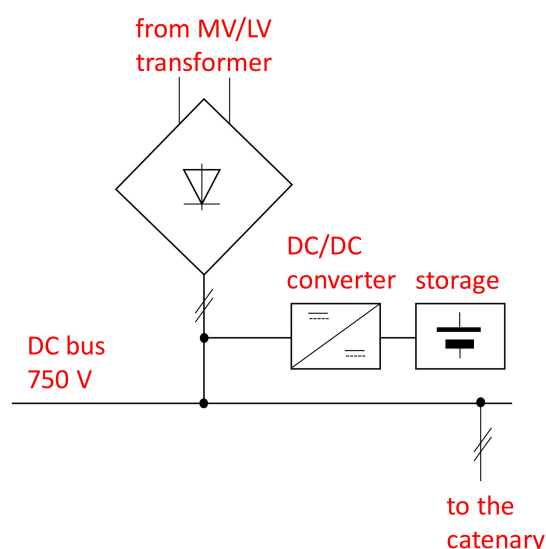


Figure 4. Scheme of the ESS equipped with storage system.

Table 6. Storage system sizing.

Technology	LFP	LTO
Nominal cell voltage (V)	32	2.4
Nominal cell capacity (Ah)	160	10
Max allowed charging current (A/Ah)	6	60
Cost (€/kWh)	150	600
Number of cells in series	190	254
Number of cells in parallel	1	5
Nominal battery capacity (Ah)	160	50
Nominal battery energy (kWh)	97.3	30.5

According to manufacturer indications [18], the maximum allowed charging cell current is extremely higher for LTO, which value has been calculated from the declared input power, fixed at 1500 W. It must also be said that the LFP manufacturer [17] does not give precise indications regarding

performance in the case of charging pulses, which have been prudently fixed to 6 A/Ah, with respect to 10 A/Ah declared for discharging pulses. Finally, cell costs have been estimated from experience by the authors [8].

The sizing of the battery pack was made having as reference the peak of charging current, which the battery is subjected during the train braking phases, i.e., about 1000 A with 10 trains on the line corresponding to a rush hour. How visible from the last rows of Table 6, the 160 Ah-capacity selected for the LFP cell perfectly matches this performance requirement. However, the capacity has to be selected also to guarantee a corresponding SOC variation compatible with the expected life of that battery. In this way, the number of charging-discharging cycles, having every day up to 10 trains on the line, which are continuously engaged in acceleration and braking phases, can reach hundreds of thousands in a few years. This solicitation can be sustained from the battery only when the corresponding SOC variation during cycling is within the range 5–10% [20–22]. In the case of the LFP solution, because of their worst performance, SOC variation under this condition must not overcome 5%. Regarding the LTO solution, although a smaller capacity would be acceptable as well regarding the maximum stress required, a capacity of at least 50 Ah is needed to stay within the indicated SOC variation, to preserve the battery life. Moreover, different lithium cell technologies (e.g., NMC, NCA, etc.) could at least be used in theory; however, as first approximation their general characteristics can be aligned to the typologies here described, and their performance within the considered range, mainly LTO oriented when able to sustain high charging/discharging current rates. An additional example describing the utilization of high-power batteries is detailed in [23].

The quantity of the braking energy to be recovered in the different scenarios was analyzed by means of a simulation tool developed in Modelica language [24] in order to evaluate the power and energy flows on the overall system. In this way, the supply network, the catenary, and the trains running have been simulated, following the same approach as in [6,25].

The tool was then validated by the utilization of the daily and annual energy flows, respectively shown in Tables 3 and 4. Obviously, daily energy flows have made it possible to correctly calibrate the ESS model parameters, the braking energy control strategy and the trains energy consumptions, by setting the maximum allowed speed along the different sections of the route, and the different mix of auxiliary loads. In this way, the tool was able to be aligned with the indicated energy required for traction in the last row of Table 4, with a gap of about 1%.

Once validated, the tool was to evaluate the energy saving gained from the installation of storage systems, from one up to ten, e.g., one for each ESS. Energy saving was evaluated as difference between the total energy delivered by the ESSs in the configuration without storage, and the total energy delivered by the ESSs in the configuration with the number of the storage systems examined. Results, taken from [9] for clarity, are in the next Table 7.

Table 7. ESSs energy demand for traction and related energy saving, for different storage systems option.

Case	Energy Delivered by the ESSs (MWh/y)	Energy Saving (MWh/y)
Base (no storage)	2756	-
1 Storage system	2604	180
3 Storage systems	2088	696
5 Storage systems	1805	979
10 Storage systems	1680	1104

It is apparently questionable if the storage sizing needs to be updated when the number of storages rises up from one up to ten units. In fact, at equal number of trains, power, and energy flows to be managed would be shared in a larger number of storages; thus, allowing a downsizing in terms of nominal capacity. However, it is also possible to observe how the need to preserve the SOC fluctuation within a narrow band, makes the choice of maintaining the original storage sizing. This is visible also

in the next Figure 5, where battery current and SOC are shown in the case of ten storage systems, for which LTO technology has been chosen. As said before, current peaks do not overcome 1000 A, and SOC variation is about 10%. Figure 5 refers to the case of a rush hour, with 10 trains running.

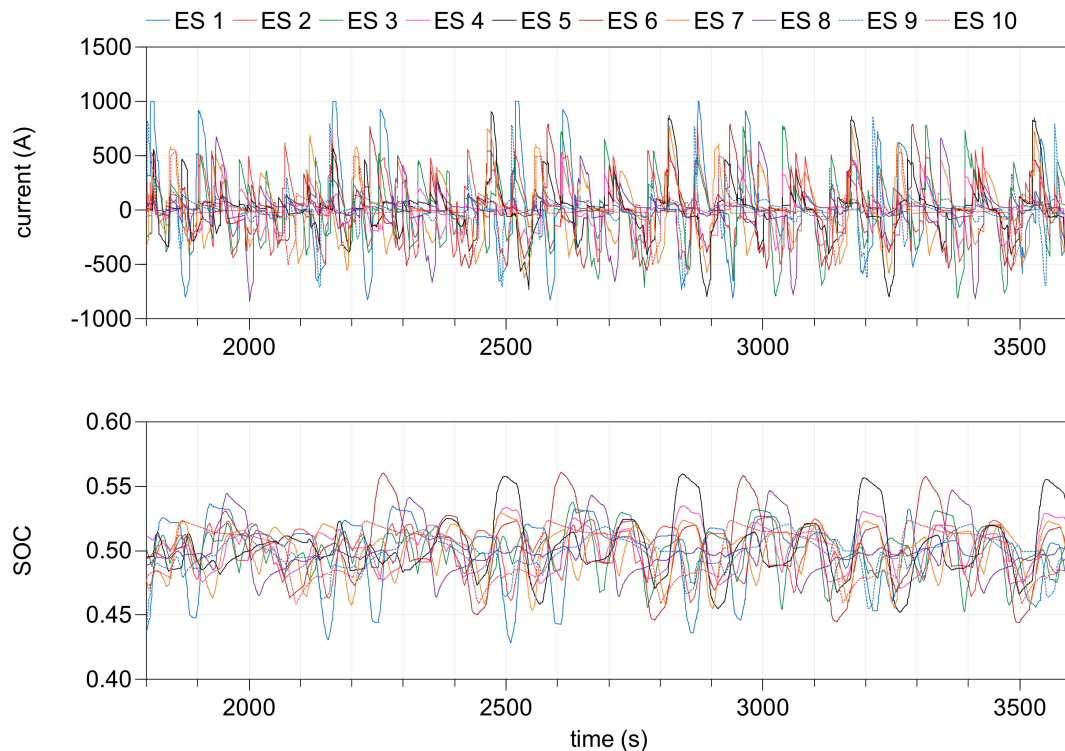


Figure 5. Battery current and SOC when having 10 storage systems installed, rush hour (ten trains running).

5.2. System Reliability

From the numbers of Table 7, it is clear that the best choice from the energy saving point of view is the installation of three storage systems; in fact, further energy saving due the increment of the storage systems up the three units cannot be compensated by their extra-purchase costs. Some sensitive analysis for different scenarios, including different costs of electricity and storage technologies are detailed in [8]. However, installation up to 10 storage systems, although less cost-efficient, may be useful as well in order to improve the system reliability. In this regard, two possible failures have to be considered:

The first failure typology takes into consideration that all the ESSs are subjected to blackout, with the electrical feeding from the grid immediately stopped. In this way, each storage system installed must serve one train on average, allowing it to reach at least two nearest subsequent train stops. This means, by considering the sequence of train stops of the previous Figure 2, each train has to cover under these conditions a traveled distance not higher than 3 km.

From simulation results, the traction energy consumption at constant speed is in the range 2.6–3.2 kWh/km for the trains running at 50 or 70 km/h respectively. Therefore, the two considered configurations were checked. In this way, considering a mid SOC level and running at the highest speed (i.e., 70 km/h), each battery pack can move at the maximum constant speed (i.e., 70 km/h) the train for about 4.8 km or 15.2 km, respectively. Therefore, the requirement to let each train running to the nearest station has been fully met.

As second failure, it has been considered the situation in which one single ESS stops working. The failure can affect or not the stationary storage, installed in parallel. In this case, no change in normal operation is allowed, to guarantee the business continuity for the service. Naturally, both the two storage configurations have been simulated. The matrix shown in the next Table 8 shows

all the considered case studied, which simulate a failure at the beginning, in the middle or at the end of the pattern, in which electrical feeding substations (ESSs) are numbered from 1 (e.g., David, see Figure 2) to up to 10 (e.g., Albino, see Figure 2). When the failure of the storage is included, it is indicated in the corresponding row, always in Table 8. Table 8 shows results from simulation outputs in terms of functionality, indicating when service interruption (-) or business continuity (x) occur, in correspondence with the hypothesized failures.

Table 8. Matrix of test cases, failure of one ESS including storage or not, for different storage systems option; business continuity (x), service interruption (-).

Failure	LFP Storage	LTO Storage
ESS1	x	x
ESS1; storage 1	-	-
ESS5	x	x
ESS5; storage 5	x	x
ESS10	x	X
ESS10; storage 10	-	-

In this way, the following main remarks can be achieved. First of all, when the failure involves both the ESS and the corresponding storage, the business continuity cannot be guaranteed in each condition, if the reference power of 1 MW is installed for each ESS. In fact, due occasional overlap of acceleration and running phases of multiple trains in the same portion of the track, power peaks delivered from the ESS can reach a maximum value nearly about 1.6 MW. This is visible in the plot of the next Figure 6, where the maximum power from ESS1 is shown, in the case of all ESSs perfectly working, or when a failure concerns the nearest ESS0. How visible, the maximum extra-peak to be supplied is about 400 kW, and it remains sustainable when the full power of 2.2 MW is yet available, i.e., with standard transformers, or with two AMT transformers installed in parallel (see Section 4.2).

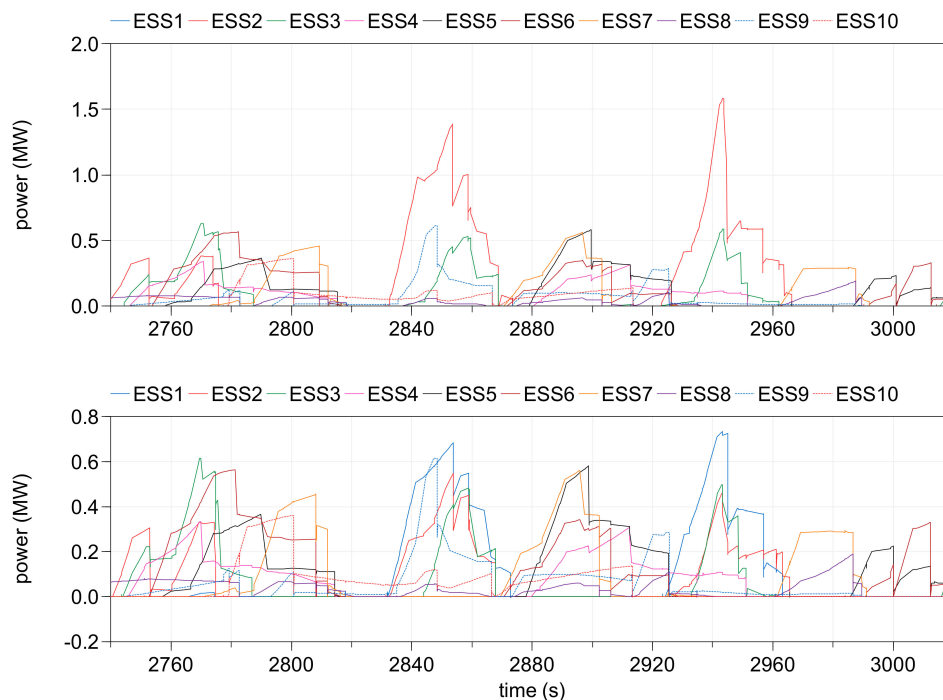


Figure 6. Power delivered from ESSs, in the case of failure from ESS1 (top) or no failure (bottom).

On the other hand, when half-power transformers having 1.1 MW are used, the extra-power needed has to be provided by the storage systems, and losses decrease from 4.5 kW and 17.5 kW (see Table 2), at exactly the half value, i.e., 2.3 kW and 8.8 kW, respectively; thus, further reducing the amount of losses calculated in the Section 4.2.

In particular, stationary storage systems are mandatory, in order to guarantee the extra-power needed. The two storage systems may appear useful as well, although the LTO configuration is properly designed for delivering high current rates, while the LFP configuration is exploited at its maximum performance, having about 600 kW delivered, aligned to the maximum allowed current rate of 6 A/Ah. Finally, when no overlap happens among multiple trains running, the business continuity is guaranteed also in the presence of a failure concerning both the storage and the feeding substation; this is the case when the failure refers to ESS4 and ESS9, always in Table 8.

6. Conclusions

This paper has described how it is possible to improve electrical feeding substations, by changing transformer technology and by installing dedicated high-power oriented storage systems.

In particular, a considerable reduction in losses up to 58% has been performed by simply changing the transformer technology, which guarantee a cost of ownership significantly lower than the standard transformer solution. Additionally, further losses reduction is obtainable by introducing half-power transformers.

Then, installation of storage systems was analyzed also by considering the improvement in terms of system reliability, in addition to energy efficiency. Results have shown also that installation of the storages is able to guarantee different tramway services, also when reducing the sizing of the installed transformers. Moreover, this last aspect can also compensate the extra-costs for the storages.

The presented results are produced on a specific case study, which represents a typical configuration for very common tramway systems and trolleybuses. Since significant similarities can be identified regarding the technical characteristics of these systems, it is therefore to be expected that the highlighted benefits from the proposed changes are nearly the same by moving from one system to another.

Author Contributions: Conceptualization, G.L., R.G., and L.S.; methodology, G.L., R.G., and L.S.; software, G.L. and L.S.; validation, G.L., R.G., and L.S.; formal analysis, G.L., R.G., and L.S.; investigation, G.L., R.G., and L.S.; resources, G.L., R.G., and L.S.; data curation, X.X.; writing—original draft preparation, G.L. and L.S.; writing—review and editing, G.L., R.G., and L.S.; visualization, G.L., R.G., and L.S.; supervision, R.G.; project administration, L.S.; funding acquisition, L.S. All authors have read and agreed to the published version of the manuscript.

Funding: This research was co-financed under Tuscany POR CREO 2014-2020 Project “FAT” (CUP 7165.24052017.112000040).

Conflicts of Interest: The authors declare no conflict of interest.

Abbreviations

The following abbreviations are used in this manuscript:

ESS	electrical feeding substation
AMT	amorphous core transformer
LV	low voltage
MV	medium voltage
RGO	gular grain-oriented
SOC	state of charge
TOC	total owning cost
LFP	lithium ferro-phosphate
LTO	lithium-titanate battery
NMC	nickel manganese cobalt oxide
NCA	lithium nickel cobalt aluminum oxide

References

1. Gonzalez-Gil, A.; Palacin, R.; Batty, P.; Powell, J. A systems approach to reduce urban rail energy consumption. *Energy Convers. Manag.* **2014**, *80*, 509–524. [[CrossRef](#)]
2. Gonzalez-Gil, A.; Palacin, R.; Batty, P. Sustainable urban rail systems: Strategies and technologies for optimal management of regenerative braking energy. *Energy Convers. Manag.* **2013**, *75*, 374–388. [[CrossRef](#)]
3. Lamedica, R.; Ruvio, A.; Galdi, V.; Graber, G.; Sforza, P.; Guidi Buffarini, G.; Spalvieri, C. Application of battery auxiliary substations in 3 kV railway systems. In Proceedings of the AEIT International Annual Conference (AEIT 2015), Naples, Italy, 14–16 October 2015; pp. 1–6.
4. Capasso, A.; Gannini, G.; Lamedica, R.; Ruvio, A. Eco-friendly urban transport systems. Comparison between energy demands of the trolleybus and tram systems. *Ing. Ferroviaria* **2014**, *69*, 329–347.
5. Roch-Dupré, D.; Cucala, A.P.; Pecharron, R.R.; Lopez-Lopez, A.J.; Fernandez-Cardador, A. Evaluation of the impact that the traffic model used in railway electrical simulation has on the assessment of the installation of a Reversible Substation. *Int. J. Electr. Power Energy Syst.* **2018**, *102*, 201–210. [[CrossRef](#)]
6. Barsali, S.; Bolognesi, P.; Ceraolo, M.; Funaioli, M.; Lutzemberger, G. Cyber-Physical Modelling of Railroad Vehicle System using Modelica Simulation Language. In Proceedings of the Second International Conference on Railway Technology: Research, Development and Maintenance, Ajaccio, France, 8–11 April 2014; pp. 1–18.
7. Capasso, A.; Ceraolo, M.; Lamedica, R.; Lutzemberger, G.; Ruvio, A. Modelling and simulation of electric urban transportation systems with energy storage. In Proceedings of the IEEE 16th International Conference on Environment and Electrical Engineering (EEEIC), Florence, Italy, 7–10 June 2016; pp. 1–5.
8. Ceraolo, M.; Giglioli, R.; Lutzemberger, G.; Bechini, A. Cost effective storage for energy saving in feeding systems of tramways. In Proceedings of the IEEE International Electric Vehicle Conference (IEVC), Florence, Italy, 17–19 December 2014; pp. 1–6.
9. Fioriti, D.; Giglioli, R.; Lutzemberger, G.; Poli, D. Storage operation in tramway systems delivering grid services. In Proceedings of the IEEE 18th International Conference on Environment and Electrical Engineering (EEEIC), Palermo, Italy, 12–15 June 2018; pp. 1–6.
10. Harlow, J.H. *Electric Power Transformer Engineering*, 3rd ed.; CRC Press: Boca Raton, FL, USA, 2013; ISBN 9781439856291.
11. Steinmetz, T.; Cranganu-Cretu, B.; Smajic, J. Investigations of no-load and load losses in amorphous core dry-type transformers. In Proceedings of the XIX International Conference on Electrical Machines (ICEM 2010), Rome, Italy, 6–8 September 2010; pp. 1–6.
12. Gatta, F.M.; Geri, A.; Maccioni, M.; Maiolini, C.; Paulucci, M.; Palone, F.; Cannavale, G.; Scaggiante, M. Impact of the recent EU regulation on HV/MV transformers: Possible technical-economic benefits arising from the replacement of old transformers. Two case studies. In Proceedings of the IEEE 16th International Conference on Environment and Electrical Engineering (EEEIC), Florence, Italy, 7–10 June 2016; pp. 1–6.
13. Carlen, M.; Xu, D.; Clausen, J.; Nunn, T.; Ramanan, V.R.; Getson, D.M. Ultra High Efficiency Distribution Transformers. In Proceedings of the IEEE PES Transmission and Distribution Conference and Exposition (IEEE PES T&D 2010), New Orleans, LA, USA, 19–22 April 2010; pp. 1–7.
14. Yurekten, S.; Kara, A.; Mardikyan, K. Energy efficient green transformer manufacturing with amorphous cores. In Proceedings of the International Conference on Renewable Energy Research and Applications (ICRERA), Madrid, Spain, 20–23 October 2013; pp. 534–536.
15. De Lucia, M.; Messeri, M. Method and Device for Manufacturing Transformers with a Core Made of Amorphous Material, and Transformer thus Produced. WO Patent 2016/142504, 15 September 2016.
16. IEEE Standards Association. *IEEE Guide for Loss Evaluation of Distribution and Power Transformers and Reactors, IEEE Std C57.120-2017 (Revision of IEEE Std C57.120-1991)*; IEEE: New York, NY, USA, 2017; pp. 1–53.
17. Winston Official Site, Prismatic LFP Cell. Available online: <http://en.winston-battery.com/index.php/products/power-battery/category/lithium-ion-power-battery> (accessed on 27 July 2020).
18. Toshiba Official Site, High Power Prismatic LTO Cell. Available online: <https://www.scib.jp/en/product/cell.htm> (accessed on 27 July 2020).
19. Simcenter Magnet Software Official Site. Available online: <https://www.plm.automation.siemens.com/global/it/products/simcenter/magnet.html> (accessed on 27 July 2020).

20. Kabitz, S.; Gerschler, J.B.; Ecker, M.; Yurdagel, Y.; Emmermacher, B.; André, D.; Mitsch, T.; Sauer, D.U. Cycle and calendar life study of a graphite $\text{LiNi}_{1/3}\text{Mn}_{1/3}\text{Co}_{1/3}\text{O}_2$ Li-ion high energy system. Part A: Full cell characterization. *J. Power Source* **2013**, *239*, 572–583. [[CrossRef](#)]
21. Ecker, M.; Nieto, N.; Kabitz, S.; Schmalstieg, J.; Blanke, H.; Warnecke, A.; Sauer, D.U. Calendar and cycle life study of $\text{Li}(\text{NiMnCo})\text{O}_2$ -based 18650 lithium-ion batteries. *J. Power Source* **2014**, *248*, 839–851. [[CrossRef](#)]
22. Omar, N.; Monem, M.A.; Firouz, Y.; Salminen, J.; Smekens, J.; Hegazy, O.; Gaulous, H.; Mulder, G.; Van den Bossche, P.; Coosemans, T.; et al. Lithium iron phosphate based battery—Assessment of the aging. *Appl. Energy* **2014**, *113*, 1575–1585. [[CrossRef](#)]
23. Antonelli, M.; Ceraolo, M.; Desideri, U.; Lutzemberger, G.; Sani, L. Hybridisation of rubber tired gantry (RTG) cranes. *J. Energy Storage* **2017**, *12*, 186–195. [[CrossRef](#)]
24. Fritzson, P. *Introduction to Modeling and Simulation of Technical and Physical Systems with Modelica*, 1st ed.; Wiley-IEEE Press: New York, NY, USA, 2011; ISBN 9781118094259.
25. Ceraolo, M.; Funaioli, M.; Lutzemberger, G.; Pasquali, M.; Poli, D.; Sani, L. Electrical Storage for the Enhancement of Energy and Cost Efficiency of Urban Railroad Systems. In Proceedings of the Second International Conference on Railway Technology: Research, Development and Maintenance, Ajaccio, France, 8–11 April 2014; pp. 1–17.



© 2020 by the authors. Licensee MDPI, Basel, Switzerland. This article is an open access article distributed under the terms and conditions of the Creative Commons Attribution (CC BY) license (<http://creativecommons.org/licenses/by/4.0/>).